Article

Design of a DNA-programmed plasminogen activator.

Purba Mukherjee, Luke J. Leman, John H. Griffin, and M. Reza Ghadiri

J. Am. Chem. Soc., **Just Accepted Manuscript** • DOI: 10.1021/jacs.8b10166 • Publication Date (Web): 22 Oct 2018

Design of a DNA-programmed plasminogen activator.

Purba Mukherjee†, Luke J. Leman†, John H. Griffin‡, M. Reza Ghadiri†, §*

† Department of Chemistry, The Scripps Research Institute, La Jolla, CA 92037, United States

‡ Department of Molecular Medicine, The Scripps Research Institute, La Jolla CA 92037, United States

§ The Skaggs Institute of Chemical Biology, The Scripps Research Institute, La Jolla, CA 92037, United States

ABSTRACT: Although the functional specificity and catalytic versatility of enzymes have been exploited in numerous settings, controlling the spatial and temporal activity of enzymes remains challenging. Here we describe an approach for programming the function of streptokinase (SK)—a protein that is clinically used as a blood "clot buster" therapeutic. We show that the fibrinolytic activity resulting from the binding of SK to the plasma proenzyme plasminogen (Pg) can be effectively regulated (turned "OFF" and "ON") by installing an intrasteric regulatory feature using a DNA-linked protease inhibitor modification. We describe the design rationale, synthetic approach, and functional characterization of two generations of intrasterically-regulated SK-Pg constructs and demonstrate dose-dependent and sequence-specific temporal control in fibrinolytic activity in response to short predesignated DNA inputs. The studies described establish the feasibility of a new enzyme-programming approach and serves as a step toward advancing a new generation of programmable enzyme therapeutics.

INTRODUCTION

Homeostasis in the cardiovascular system is achieved through a finely tuned, intrinsic balance between the coagulation cascade and the fibrinolytic/thrombolytic pathways.[1] Dysregulation of these coordinated networks can occur due to genetic and lifestyle factors, resulting in diverse pathologies including life-threatening cardiovascular conditions such as myocardial infarction, ischemic stroke, and pulmonary embolism, the leading causes of non-communicable deaths.[2,3] The discovery and development of "clot buster" therapeutics (thrombolytic agents) derived from natural plasminogen activators (PAs) has been an indispensable clinical tool for managing acute thrombotic events. PAs are key to the fibrinolytic cascade and initiate clot dissolution by the proteolytic processing of plasminogen (Pg).[4] This converts Pg from its single-chain zymogen form to its two-chain, enzymatically active form, plasmin (Pm). Pm then proteolytically digests the insoluble fibrin mesh that makes up blood clots. There are two endogenous PAs in humans, tissue-type plasminogen activator (tPA) and urinary-type plasminogen activator (uPA), which share the ability to activate Pg but differ in their biological roles.[5–8]

Pathogenic streptococci bacteria produce a PA called streptokinase (SK) that hijacks the fibrinolysis cascade. Contrary to its nomenclature, this protein lacks enzymatic activity. Rather, it binds stoichiometrically to Pg, which induces a conformational change in Pg to form an enzymatically active SK-Pg* complex.[9,10] SK-Pg* then proteolytically cleaves other circulating Pg molecules to convert them into active Pm, initiating fibrinolysis (Figure 1). SK was the first Pg activator to be approved for clinical use, and although its use as a therapeutic has been largely replaced by tPA in developed nations, SK remains essential for managing acute myocardial infarction in developing countries.[11,12]

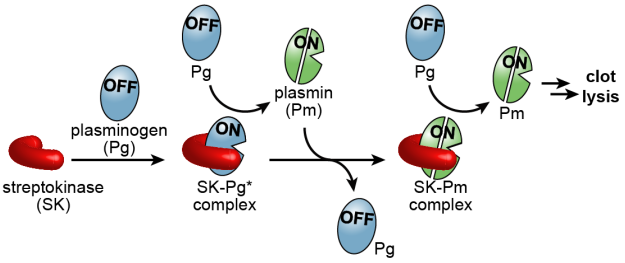

Figure 1. Overview of streptokinase-mediated activation of fibrinolytic cascade. Association of streptokinase (SK) with plasminogen (Pg) triggers a conformational change in Pg to generate an enzymatically active SK-Pg* complex, which can proteolytically process substrate Pg to plasmin (Pm). Pm formed in this way undergoes exchange with SK-bound Pg to further accelerate Pm production. Plasmin then cleaves the insoluble fibrin mesh resulting in the dissolution of blood clots.

One challenge associated with SK as a therapeutic is that its mode of action leads to indiscriminate, systemic Pm generation and a drastic depletion of circulating Pg and alpha 2-antiplasmin. This, in turn, causes significantly reduced blood clotting capacity and substantial risk of intracranial hemorrhages.[3] We hypothesized that if the extent, timing, and site of enzymatic activity of SK-Pg* could be better controlled, it might be possible to mitigate some

of the liabilities associated with SK. Here we describe our first steps toward that goal of programming PA activity by employing the principles of intrasteric regulation.

Intrasteric regulation is a ubiquitous process used by a variety of enzyme classes such as proteases, kinases, and phosphatases.[13,14] At the molecular level, the intrasteric regulation of an enzyme is typically achieved by an appended C- or N-terminal pseudosubstrate that prohibits access to the active site. Regulation occurs at the allosteric site of the complex, the site between the enzyme and pseudosubstrate, where a conformational change or cleavage event releases the pseudosubstrate from the active site (Figure 2). A well-studied example is that of twitchin kinase where the binding of the activator protein S100A1 to the allosteric site induces a conformational change that activates the enzyme.[15] Another attractive feature of intrasteric regulation is the potential modularity of the allosteric site, which can be engineered to respond to other binding or cleavage events.[16]

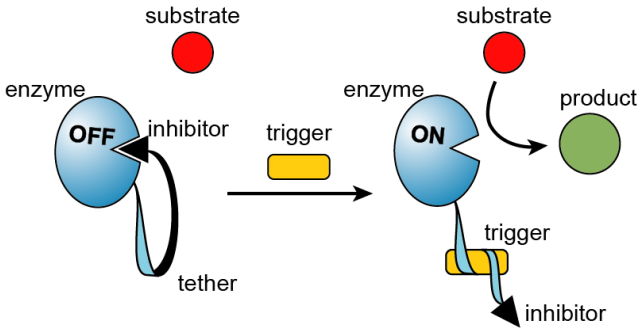

Figure 2. General scheme of an intrasterically-regulated enzyme and its mechanism of activation. Sufficiently strong binding interactions of a molecular trigger to the allosteric tether induces a conformational change that liberates the inhibitor or pseudosubstrate from the enzyme active site. Alternatively, the tether can be cleaved to reactivate the enzymatic function (such as seen in caspase activation). The activated enzyme amplifies the trigger recognition event by turning over multiple substrates to generate an output signal.

We have previously established a semi-synthetic approach to programming enzyme activity. The key aspect of the design is the covalent attachment of an enzyme to its small molecule inhibitor through a DNA tether. This action turns an intermolecular inhibitor into an intramolecular one, resulting in a high effective concentration of the inhibitor at the active site[17] and forcing the enzyme into an inactive state ("OFF" state). Moreover, a judicial choice of a nucleic acid tether (allosteric modulator) enables site- and sequence-specific programming of enzyme activity.[18–21] For instance, the addition of a complementary DNA strand can restore the enzyme activity ("ON" state) as a result of sequence-specific DNA hybridization (duplex formation) altering the DNA tether structure and mechanically forcing the inhibitor out of the enzyme active site. This basic concept has been extended to several design architectures and programming options, such as turning enzymes ON and OFF and logic operations.[18,19,21]

Here, we show that DNA-programmed intrasteric regulation can be extended to modulate the activity of protein-protein complexes (Figure 3). SK binding to Pg

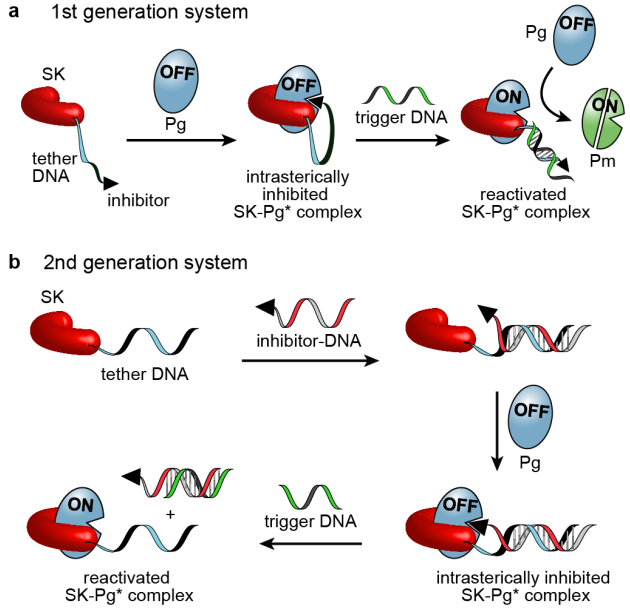

Figure 3. Schematic diagram of intrasterically-regulated SK-Pg* complexes. We constructed two distinct architectures of DNA-programmed SK constructs. In both designs, a small molecule Pm inhibitor is held in close proximity to the active site of the SK-Pg* complex via a DNA tether. Upon interaction of the tether with a complementary DNA trigger strand (duplex formation), the ensuing rigidification of the tether reactivates the enzyme by dislodging the inhibitor from the active site. (a) The 1st generation construct is composed of a Pm inhibitor attached directly to SK via a DNA tether strand. (b) The 2nd generation design involves the Pm inhibitor being noncovalently attached to SK through a DNA duplex, which provided for a more convergent synthesis and added flexibility in design and functional aspects.

induces a conformational change in Pg that creates a serine protease-type active site arrangement (Pg*) capable of cleaving and activating free Pg to Pm, thus initiating the fibrinolytic cascade (Figure 1). We hypothesized that a SK semi-synthetic construct bearing a Pm inhibitor that is covalently attached at an appropriate site on the protein via a DNA tether, could bind to Pg and result in a pseudo-intramolecular inhibition of the SK-Pg* active site (Figure 3a). Such a protein-protein complex (SK-Pg*-DNA-inhibitor) should remain in the OFF state until reactivated on demand by the introduction of a complementary DNA trigger strand (Figure 3a). We have explored two distinct architectures of DNA-programmed, intrasterically-regulated SK constructs and demonstrate that these enable controlled initiation of the fibrinolytic cascade (Figure 3a,b). In the 1st generation architecture, the inhibitor was covalently linked to SK through a short, single-stranded DNA tether (Figure 3a). In contrast, in the 2nd generation design, the inhibitor is noncovalently attached to SK through a DNA duplex involving two complementary tether strands, one appended to SK and the other linked to the inhibitor (Figure 3b). The advantage of the 1st generation design is simplicity. However, construction of 1st generation architecture requires several sequential synthetic and purification steps to generate each new construct. In contrast, the 2nd generation architecture is more convergent synthetically and more flexible in several functional aspects. For example, in the 2nd generation

architecture, the DNA sequences that position the inhibitor near the active site of the SK-Pg* complex can be optimized independently of the DNA sequences in the regions responsible for activation, and the 2nd generation architecture provides multiple possible modes of reactivation[18]. As described below, both of these design architectures proved effective in enabling DNA-mediated programming of PA activity.

RESULTS AND DISCUSSION

Mutant enzyme production. Our synthetic strategy required site-specific coupling of a DNA tether to SK. To do this, we exploited the absence of cysteine residues in wild type SK. From a model of the SK-Pg*-Pg complex constructed from existing structures of SK, Pg, and their co-complex (Figure S1)[22–24], we chose six solvent exposed residues (E75, K76, A77, Q152, N153 and Q154) as potential sites for mutation to cysteine and attachment of the DNA tether. The choice of amino acid mutation site was based on the criteria that the position must be (i) located on the surface, (ii) should not have vital inter- or intramolecular interactions, and (iii) was within reach of the SK-Pg* active site to allow unobstructed access of the DNA-tethered inhibitor. We expressed and purified wild type recombinant SK (rSK) and two Cys mutants (E75C and Q152C). The activity and kinetic characteristics (k_{cat} and K_M) of the Q152C mutant were measured and found to be comparable to those of rSK (Table 1), as determined by *in vitro* assays[25,26] that measure cleavage of the chromogenic peptide substrate S2251 (Table 1a) or cleavage/enzymatic activation of SK's natural substrate, Lys-plasminogen (Lys-Pg) (Table 1b).

Table 1. Observed SK-Pg* steady-state kinetic parameters for WT recombinant SK and its variants in: a) hydrolysis of chromogenic peptide substrate S2251 (D-Val-Leu-Lys-p-nitroanilide), and b) proteolytic activation of Lys-plasminogen (Lys-Pg).

a

SK construct	k_{cat} (s^{-1})	K_M (μM)	*Efficiency* (k_{cat}/K_M) ($x10^6\ M^{-1}s^{-1}$)
rSK	25.7 ± 1.5	410 ± 80	0.063
Q152C	23.6 ± 0.9	400 ± 50	0.059
Q152C-D2	23.1 ± 1.3	930 ± 120	0.025
Q152C-D3	29.2 ± 1.1	850 ± 80	0.034
Q152C-DE	30.9 ± 0.9	900 ± 60	0.034

b

SK construct	k_{cat} (s^{-1})	K_M (nM)	*Efficiency* (k_{cat}/K_M) ($x10^5\ M^{-1}s^{-1}$)
rSK	0.162 ± 0.01	450 ± 110	3.6
Q152C	0.128 ± 0.01	370 ± 140	3.45
Q152C-D2	0.340 ± 0.02	700 ± 120	4.8
Q152C-D3	0.262 ± 0.01	730 ± 80	3.58
Q152C-DE	0.213 ± 0.01	680 ± 80	3.11

Errors represent standard error of mean of duplicates.

Synthesis of the SK-DNA-Inhibitor constructs. Several active site inhibitors of Pm have been previously described.[8,27,28] We chose to use the peptidomimetic inhibitor CU2010 (see Figure S2 (inset) for structure) because it met our two criteria: (i) a reversible, non-covalent mechanism of inhibition, and (ii) moderate binding affinity ($K_i \approx 2$ nM) to allow subsequent DNA trigger-dependent dissociation from the active site as required for the intrasteric regulation of the SK-Pg* complex. We developed a new solid-phase strategy (Figure 4) that permitted a concise synthesis of the inhibitor and enabled the installation of an iodoacetamidyl group as a chemical handle for conjugating the inhibitor to a thiol-terminated DNA strand. The iodoacetamidyl group was introduced at a position that was thought not to affect binding to the enzyme active site, based on an examination of structural models of Pm bound to CU2010-like inhibitors.[28,29]

With an eye toward the solid-phase approach, the inhibitor was retrosynthetically broken down into a series of Fmoc-protected subunits that could be sequentially coupled to construct the molecule. 2-Chlorotrityl chloride polystyrene resin was loaded with Fmoc-3-aminomethyl-L-Phe-OAll in dry DCM and then treated with piperidine to effect Fmoc removal and provide loaded resin **1**. Carbodiimide-mediated coupling of Fmoc-D-2-amino-5-phenylpentanoic acid, followed by Fmoc removal with piperidine, afforded a resin bound dipeptide. Next, treatment with Hunig's base and Fmoc-aminomethyl phenylmethanesulfonyl chloride **4**, followed by removal of the allyl group, afforded resin-bound sulfonamide **5**. The sulfonyl chloride **4** was prepared from Boc-aminomethyl 3-(bromomethyl)benzene **2** in 61% overall yield (over 4 steps as shown). The next step of the solid-phase synthesis involved carbodiimide-mediated coupling of 4-(Boc-amidino)-benzylamine **8**, which was prepared from 4-cyanobenzyl bromide **6** (58% overall yield for 5 steps) by way of intermediate 4-amidinobenzyl azide **7**. The resulting resin-bound compound **9** was treated with piperidine to remove the Fmoc group, acylated with iodoacetic acid, and finally cleaved from the resin by treatment with TFA to afford the desired inhibitor **10** in 31% overall yield based on initial resin loading (Figure 4). We also prepared an analogous inhibitor (compound **11**) with an acetyl group in place of the iodoacetamidyl group as a control to characterize the inhibitory activity of the compound towards SK-Pg* ($K_i \approx 400$ nM) (Figure S2).

To prepare the SK-DNA-inhibitor constructs, the bifunctional maleimide-PEG-dibenzocyclooctyne (DBCO) linker **12** was coupled to the Q152C SK mutant (Figure 5), taking advantage of the chemoselective reaction between the maleimide and Cys thiol in the mutant protein. Next, one of several azide-modified DNAs (D2 or D3 for 1st generation constructs; DE for 2nd generation constructs) was conjugated to the DBCO moiety linked to the protein by strain-promoted alkyne-azide coupling (SPAAC).[30] The D2 tether contained a short hairpin that might help orient the inhibitor toward the putative active site, whereas D3

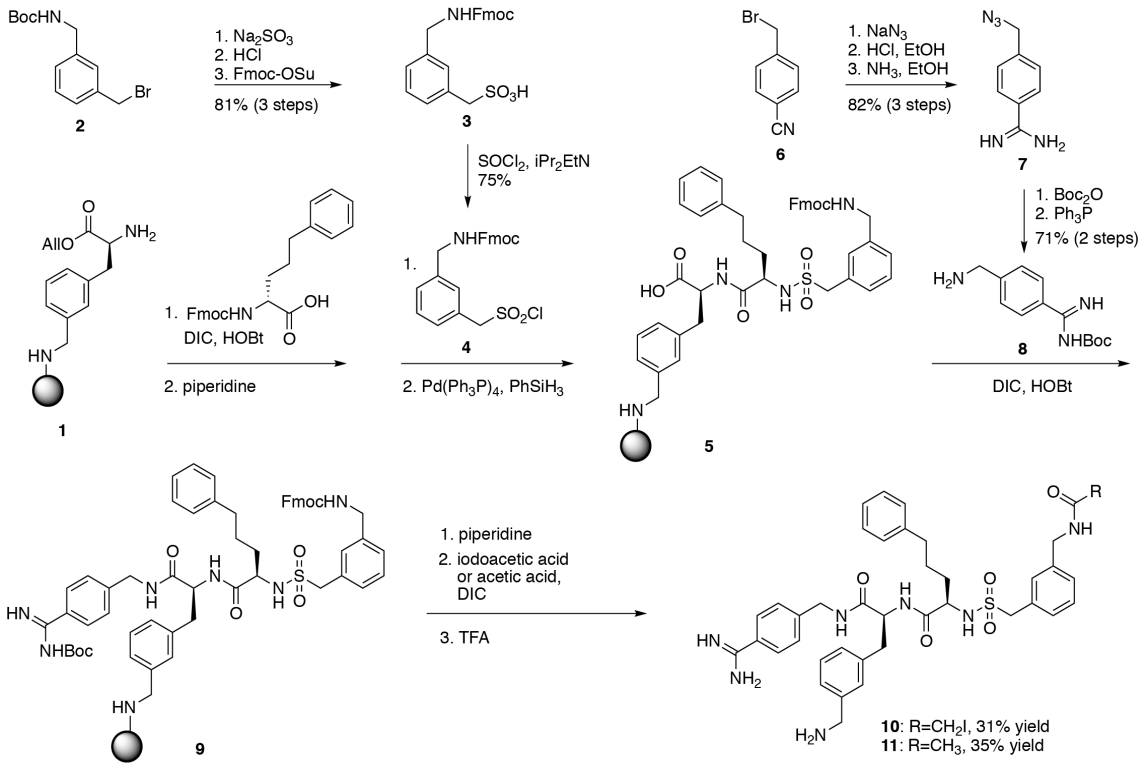

Figure 4. Solid-phase synthetic route used to prepare the Pm inhibitor component of the intrasterically-regulated constructs. All, allyl; Boc, tert-butoxycarbonyl; DIC, N,N'-diisopropylcarbodiimide; Fmoc, fluorenylmethyloxycarbonyl; HOBt, 1-hydroxybenzotriazole; OSu, N-hydroxysuccinimide; TFA, trifluoroacetic acid.

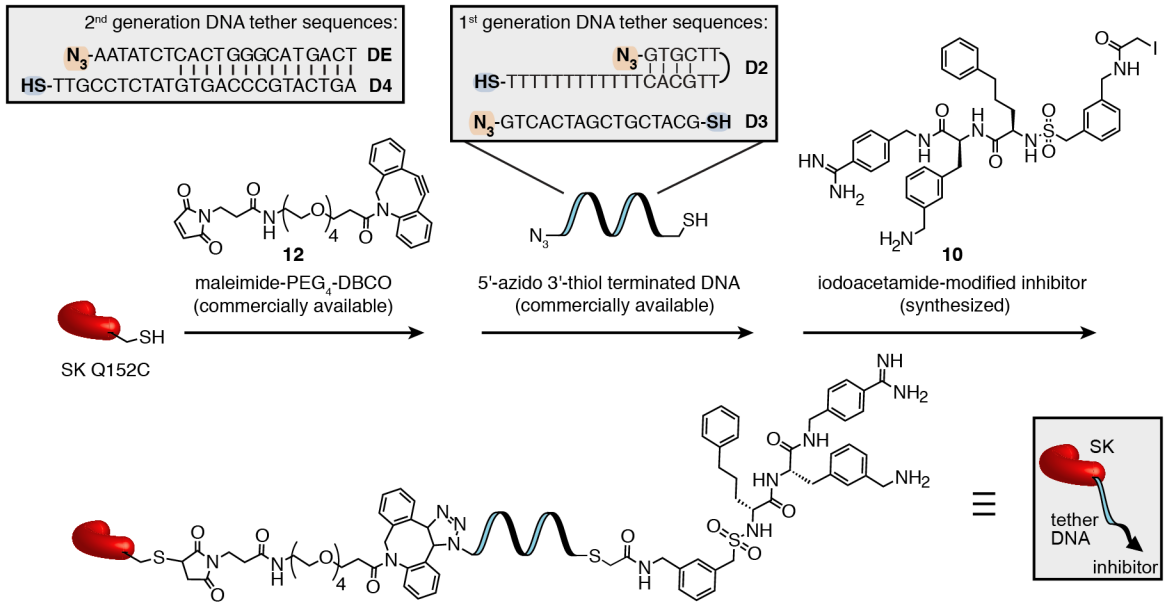

Figure 5. Synthetic route used to prepare the 1st generation SK-DNA-inhibitor construct. Not to scale. PEG, polyethylene glycol; DBCO, dibenzocyclooctyne. For 2nd generation construct preparation, a similar strategy was employed except the tether DNA was not covalently coupled to the inhibitor

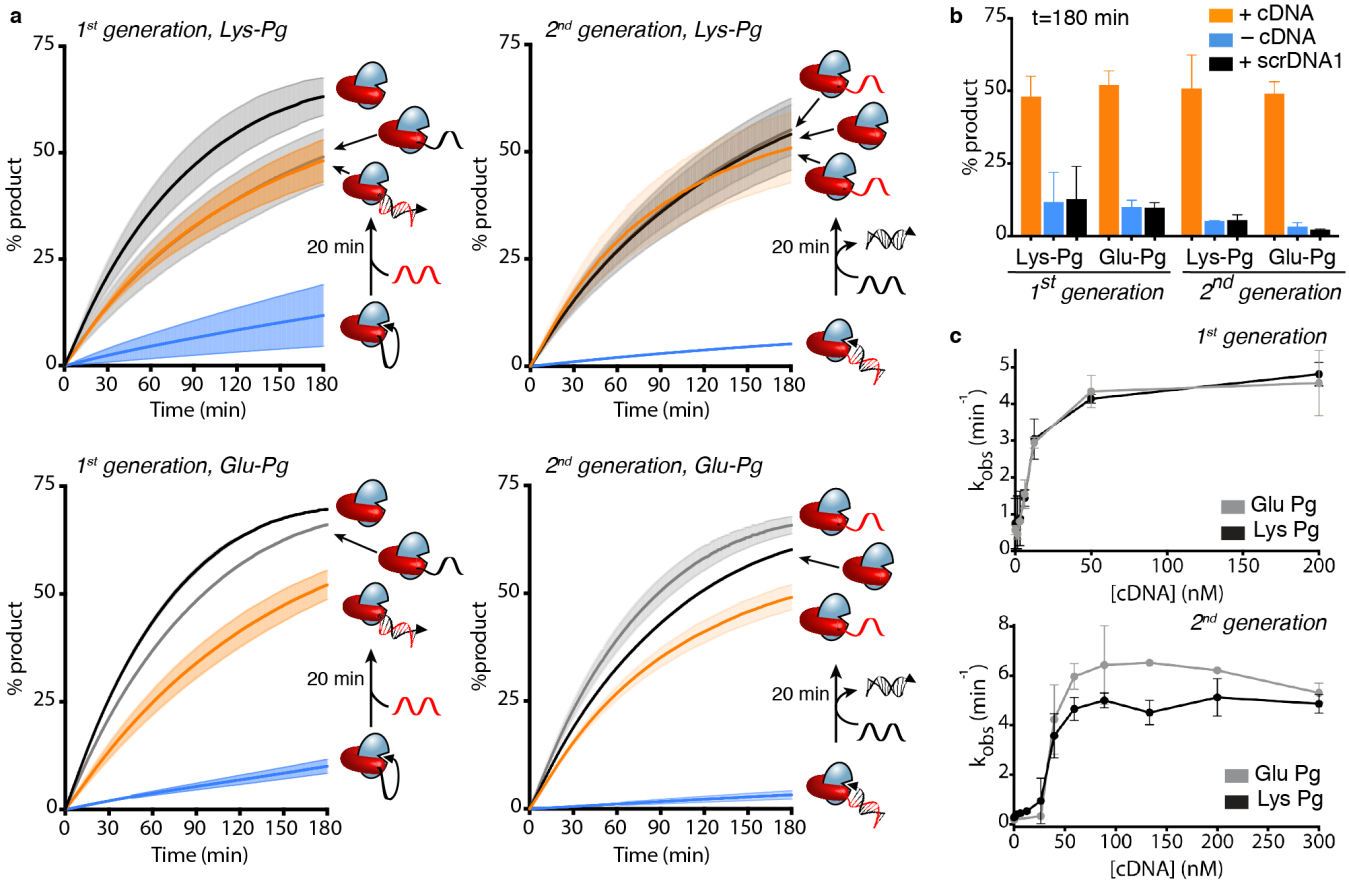

Figure 6. Functional characterization of DNA-programmed SK constructs. (a) Plots showing hydrolysis of chromogenic peptide substrate S2251 (1 mM) as mediated by various SK-Pg* complexes (10 nM) over 3 h at 37 °C. The 1st generation constructs contained the D2 DNA tether sequence and were reactivated by using a 20 min preincubation with 200 nM cDNA (D2_complement; see Table S1 for DNA sequences). The 2nd generation constructs were assembled by annealing Q152C-DE to I-D4 (1:1.5 ratio) and were reactivated by using a 20 min preincubation with 200 nM cDNA (D4_complement; Table S1). Control reactions with Q152C (black) and the appropriate DNA-conjugated Q152C (gray) are shown for each reaction. (b) Product formation after 3 h by various constructs in the absence or presence of cDNA or in the presence of scrambled DNA (scrDNA1; Table S1). DNA was used at concentrations of 200 nM and 300 nM for the 1st and 2nd generation constructs, respectively. **c** Initial rates of substrate hydrolysis (k_{obs}) by the SK-Pg* complexes with Lys- or Glu-Pg as a function of increasing trigger cDNA concentrations. The 1st generation construct Q152C-D2-Inhibitor and 2nd generation construct (DE: D4-Inhibitor= 1:1.5) were employed. Shaded regions represent error bars as SD of duplicates. All data are shown as mean ± SD of duplicate reactions.

lacked any predicted structure. Finally, inhibitor **10** was coupled smoothly to the protein-DNA conjugates (1st generation constructs) or to DNA D4 (2nd generation construct) via alkylation between the iodoacetamide handle on the inhibitor and a thiol moiety at the terminus of the DNA. Constructs were purified by ion-exchange and size exclusion chromatography (gels shown in Figure S3) and characterized by ESI-MS (see methods). As controls, we synthesized SK-DNA conjugates lacking the inhibitor moiety (Q152C-D2, Q152C-D3, and Q152C-DE). These control SK-DNA conjugates exhibited generally similar Pg-activating ability and kinetics when compared to wild type rSK or Q152C (Table 1). Attachment of the oligonucleotide tethers resulted in ≤2-fold increase in K_M and no significant effect on catalytic efficiencies (k_{cat}/K_M) for processing Lys-Pg (Table 1b). These data show that SK point mutations and DNA conjugations studied here did not significantly affect the function of SK (i.e. binding to Pg and formation of catalytically competent SK-Pg*).

Characterization of the "OFF" and "ON" states of programmed SK constructs. Successful enzyme programming requires both the ability to intrasterically inactivate the enzyme (low background) and reactivate the enzyme efficiently in a DNA trigger-dependent manner. To assess the degree of inhibition (OFF state) achieved in the designed constructs, we evaluated the level of background substrate hydrolysis for two isoforms of Pg present in circulation- Glu-plasminogen (Glu-Pg) and its amino terminal processed variant, Lys-plasminogen (Lys-Pg) (Figure 6).[31–33] Product formation fell to very low levels for the intrasterically-inhibited constructs compared to active Q152C, irrespective of the plasminogen form (prolonged incubations of 3 h resulted in only ≤10% of product formation) (Figure 6a,b), demonstrating effective control over SK-Pg* enzymatic activity. Likewise, initial rates of product formation (k_{obs}) fell by nearly 10-fold when compared to the respective tether-only variants or Q152C (Figure 6). The low level of background leakage is likely due to trace protein impurities and/or DNA degradation that could lead to the formation of active enzyme complexes.

We found that the intrasterically-inhibited SK-Pg* complexes could be efficiently turned "ON" (reactivated) in a trigger-dependent, sequence-specific fashion. To init-

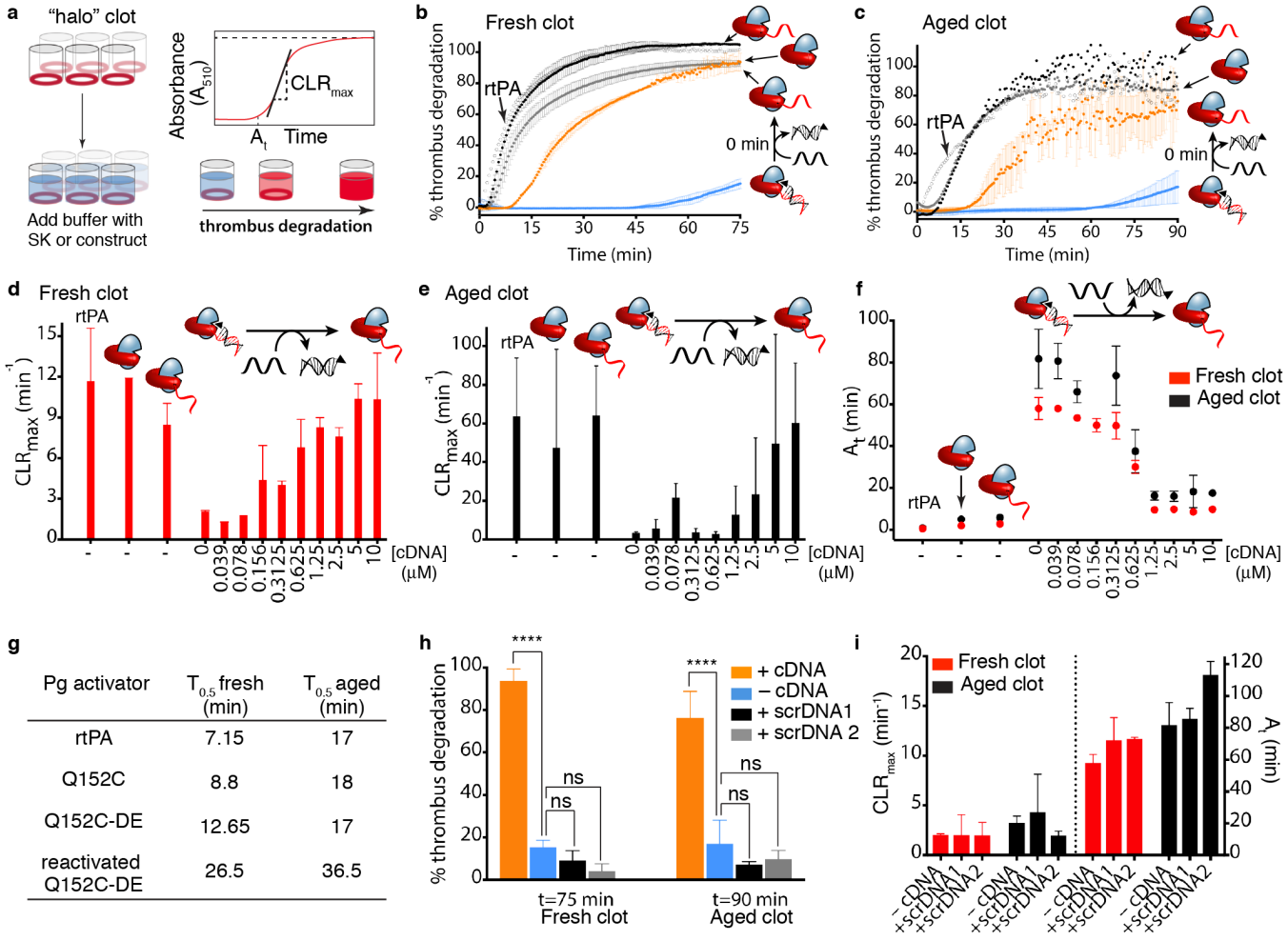

Pg activator	$T_{0.5}$ fresh (min)	$T_{0.5}$ aged (min)
rtPA	7.15	17
Q152C	8.8	18
Q152C-DE	12.65	17
reactivated Q152C-DE	26.5	36.5

Figure 7. Functional characterization of DNA-programmed SK constructs in whole blood clot lysis. (a) Schematic diagram of the assay setup and analysis. Blood was pipetted along the wall of wells in a 96-well plate, and the formation of "fresh" or "aged" clots was accomplished by adding thrombin and incubating at 37 °C for 1 h or 4 h, respectively (see Figure S7). (b,c) Time course of degradation of fresh or aged clots by Q152C-DE:I-D4 (1:10 ratio; final concentrations of each component in the assay were 100 nM:1 μM) in the absence and presence of cDNA. The cDNA was present at a concentration of 1.25 μM and 10 μM in fresh and aged clot reactions, respectively. Control reactions with Q152C, Q152C-DE and recombinant tissue-type plasminogen activator (rtPA) are also shown. Error bars represent SD of biological duplicates. For purposes of clarity error bars are only shown for inhibitor-bound constructs. (d,e) The maximum rate of clot lysis achieved during the experiment (CLRmax) was measured for the DNA-programmed SK construct (final concentration in clot=100 nM) in the presence of various concentrations of cDNA. (f) Activation times (At) observed for fresh and aged clots for various conditions. At is defined as the time required for the first derivative of the rate of product formation to rise above 1.0 min-1, and is a measure of the lag following the start of the reaction before the fibrinolytic cascade is observably initiated. Cartoon representation of constructs are shown alongside or above panel as necessary. (g) Table of time required to reach 50% clot lysis (T0.5) for each SK variant on fresh and aged clots. (h) Product levels at the assay endpoints shown in the absence or presence of cDNA or in the presence of scrambled DNAs (scrDNA1 or scrDNA2; Table S1). cDNA was used at concentrations of 1.25 μM for fresh and 10 μM for aged clots, respectively. In all cases, scrDNA was used at a concentration of 10 μM. ****, ANOVA p<0001. i Clot lysis parameters CLRmax and At for negative control reactions (dotted line separates CLRmax and At values). Error bars represent SD of biological duplicates.

iate DNA-triggered reactivation, we introduced a short DNA oligonucleotide complementary to the inhibitor-bearing strand of each construct (henceforth referred to as "cDNA") (Figure 6a,b). Duplex formation was expected to occur rapidly and proportional to the amount of cDNA present, so we varied the cDNA concentration relative to amount of intrasterically-inhibited construct. Indeed, reactivation rates increased in a dose-dependent manner with the cDNA for both 1st and 2nd generation constructs (Figure 6c, Figure S4a). The rates of substrate turnover for reactivated complexes were within 2-fold that of Q152C. Reactivation was independent of how long cDNA had been preincubated with the constructs (t_{inc}) (see Figure S5 for plots of substrate turnover with no preincubation). Likewise, activity assays indicated only a small (~2-fold) decrease in catalytic efficiency for the reactivated 1st generation constructs compared to their corresponding inhibitor-free SK constructs, even though the inhibitor remained covalently attached to the complexes (Figure S6). The expected high specificity of the trigger strand for

enzyme reactivation was confirmed by using a control, scrambled (non-complementary) DNA (scrDNA) in lieu of cDNA (see Table S1 for DNA sequences).For both generations of constructs, at scrDNA concentrations comparable to the highest [cDNA] tested, we failed to detect any activity greater than background (Figure 6b).

DNA-programmed whole blood clot lysis. We next examined the efficacy of the semi-synthetic constructs dissolving whole blood clots, a setting that better represents the complex milieu of blood that would be encountered in circulation. We employed a whole blood "halo" clot lysis assay[34] with minor modifications (see Methods) (Figure 7a, Figure S7) to assess degradation of both fresh (Figure 7b) and aged (Figure 7c) whole blood clots. These experiments were carried out using only the 2nd generation construct due to its observed lower background (Figure 6) and more convergent synthesis compared to the 1st generation designs.

Our data strongly support the effective functioning of the construct as a programmable PA in the complex environment of clotted whole blood. We found that the intrasterically-inhibited complex displayed <5% background activity up to 1 hr, whereas the reactivated construct achieved 87% thrombus degradation on fresh clots in the same time period (Figure 7). Enzyme reactivation was both dose- (Figure 7b-f) and sequence-dependent (Figure 7h-i). The efficiency of reactivation was quantified using two criteria: the maximum clot lysis rate achieved, CLR_{max} (Figure 7d-e), and time required for activation, A_t (Figure 7f). Both of these measures supported that background clot lysis was indistinguishable from negative controls in the absence of the trigger DNA strand, while exposing the system to the trigger DNA resulted in fast reactivation with a concomitant increase in CLR_{max} and decrease in A_t to levels comparable with positive control reactions (Figure 7). As negative controls, two oligonucleotides with scrambled sequences failed to reactivate the enzyme complex "OFF" state to any measurable degree above background. Because the degree of clot penetration and dissolution by thrombolytics is influenced by clot stability and maturation, we tested the functioning of the intrasterically-inhibited construct on both fresh and aged (retracted) clots (Figure 7c). As expected, clot lysis occurred at a slower rate (~6-fold) on aged clots (Figure 7c and Figure 7e), but followed the same trends observed with fresh clots. The higher inter-individual variability observed more distinctly with aged clots is due to inherent differences in the levels of blood components involved in thrombolysis, which alter how clot lysis progresses between individuals and is consistent with a previous report.[34] In both the fresh and aged whole blood clot lysis studies, we observed a lag for reactivation of the construct as compared to controls. The time required to achieve 50% clot lysis ($T_{0.5}$) by the reactivated SK-Pg* was 2–4-fold greater than reactions involving recombinant tissue-type plasminogen activator (rtPA), Q152C, or Q152C-DE (Figure 7g).

CONCLUSIONS

The studies described here represent a step toward gaining improved control over the extent, timing, and ultimately, site of PA function by employing programmable semi-synthetic protein constructs. We have characterized the effectiveness of a new design concept for harnessing the activity of SK-Pg complex and validated its efficacy in the complex environment of whole blood clots. The key feature of our approach is its novel focus on harnessing the binding partner of an enzyme as a "pseudo-domain" for establishing engineered intrasteric regulation. The repurposing of a protein's binding partner, as opposed to modifying the enzyme itself to create a programmable enzyme function, points to a more general concept for the future designs of regulated enzymes, such as the use of DNA inhibitor-modified antibodies as specific binding partners for regulating enzyme function. We hope the design principles described in this study would spur novel approaches for advancing future generations of therapeutic enzyme complexes.

EXPERIMENTAL SECTION

Expression and purification of SK: The SK-encoding gene from *Streptococcus equisimilis* (plasmid pMF1, ATCC strain 39613) was cloned into pET28b+ (Novagen) with a TEV protease cleavable N-terminal hexa-histidine (6xHis) tag. As SK lacks native cysteines, a Cys point mutant (Q152C) was generated for ease of bioconjugation. Soluble SKs (all variants described here) were expressed in Rosetta-gami2(DE3) cells (Novagen) grown in terrific broth auto-induction media (Formedium) overnight at 30°C and affinity purified utilizing the 6xHis tag that was cleaved post-purification. Tagless SK was further purified by gel-filtration and stored in protein storage buffer (50 mM sodium phosphate pH 7.5, 100 mM NaCl, 0.5 mM EDTA and 5% glycerol). Sample purity was verified using a 4-12% Bis-Tris SDS PAGE and concentrations were calculated using an ε_{280}= 38,380 $M^{-1}cm^{-1}$ for SK. Aliquots of purified SK were flash frozen and stored at -80°C. Our protein production method is an improvement over the previously reported process that required protein refolding.[26,35]

Bioconjugation and purification of Q152C-DNA-Inhibitor: Purified Q152C was reduced in the presence of 10-fold excess TCEP at 4°C for 30 mins with constant shaking. TCEP was removed using a 7kD Zeba spin desalting column (Thermo Fisher) pre-equilibrated in 2X reaction buffer (100 mM sodium phosphate pH 7.0, 200 mM NaCl, 1 mM EDTA and 10% glycerol). The desalted protein was used immediately for functionalization with excess DBCO-PEG_4-maleimide (Click Chemistry tools LLC) at 4°C for 2.5 h with shaking. Another desalting step similar to that described above removed excess labeling reagent and exchanged protein into conjugation buffer (50 mM sodium phosphate pH 8.3, 100 mM NaCl, 0.5 mM EDTA and 5% glycerol). Labeling efficiency obtained with DBCO-linker was between 85-90%.

The DBCO-conjugated Q152C was coupled via SPAAC to commercially synthesized tether DNAs (Integrated DNA technologies) (Figure 5, Table S1) overnight at 4°C with shaking. DNA conjugated protein was separated from unlabeled SK by anion-exchange chromatography

over a Mono Q 5/50GL (GE Healthcare) column using a 15-60% gradient between buffer A (50 mM sodium phosphate pH 8.3, 100 mM NaCl, 0.5 mM EDTA and 5% glycerol) and buffer B (buffer A with 1.25 M NaCl). Q152C-DNA conjugate containing fractions were concentrated using a 10kD-cutoff Amicon filter (EMD Millipore) and exchanged into protein storage buffer before storage at -80°C. Protein concentration for constructs modified with oligonucleotide was estimated using the extinction coefficient for the tether.

First generation constructs were synthesized by one of the two following methods, which differed in the order that the SK, DNA tether, and inhibitor were attached to each other. In the first approach, the disulfide at the 3' end of the oligonucleotide in Q152C-DNA was reduced using TCEP before inhibitor coupling, following the same TCEP treatment protocol as described above. After removal of the reducing agent, a 10-fold excess of compound **10** was reacted with Q152C-DNA in conjugation buffer for 30 mins, protected from light at room temperature with shaking. The thiol-group obtained post-reduction reacts with the iodoacetamide on the plasmin inhibitor (compound **10**, Figure 4) to generate the corresponding thioether. Alternatively, the reduced oligonucleotide (before being attached to Q152C) was coupled to the inhibitor under identical buffer conditions and purified by reverse phase preparative HPLC (Gemini NX5u C18 column 250 x 30 mm, Phenomenex) using a 3-50% binary gradient of 10 mM ammonium acetate, pH 8.3 and 95% acetonitrile. Pooled fractions were lyophilized and the mass of the DNA-inhibitor conjugate was confirmed by MALDI-TOF (MALDI TOF for D4-Inhibitor calcd: 8,170, M_{avg}: 8,163). These steps were identical for inhibitor containing DNAs generated for both generations. First generation constructs were prepared by subsequently coupling the inhibitor-attached strand to the protein by SPAAC as described above before purification by size-exclusion with a Superdex 10/30GL column was performed for the removal of excess inhibitor and buffer exchange of Q152C-DNA-Inhibitor obtained into protein storage buffer. The final product was verified with SDS PAGE and concentrated before storage at -80°C. ESI-MS (positive mode) was performed to verify the molecular weight of the conjugated constructs. Q152C M_{avg} calcd: 47,406, obsd: 47,409; Q152C-D2 M_{avg} calcd: 55,829, obsd: 55,849; Q152C-D2-inhibitor M_{avg} calcd: 56,552, obsd: 56,573; Q152C-D3 M_{avg} calcd: 53,408, obsd: 53,413; Q152C-D3-inhibitor M_{avg} calcd: 54,132, obsd: 54,136; Q152C-DE M_{avg} calcd: 54,804, obsd: 54,807.

Synthesis of plasmin inhibitors *10* and *11*: The plasmin inhibitor used in this study has been described before.[36,37] Here we report an alternative synthesis scheme for this peptidomimetic (Figure 4). Details of the inhibitor synthesis are mentioned in Supplementary Information.

Biochemical characterization: All reactions were performed at 37°C in reaction buffer (50 mM HEPES, pH 7.5, 125 mM NaCl, 1 mM EDTA and 1 mg/ml PEG8000) in 96-well, flat bottom NBS microplate (Corning) on a Synergy 2 plate reader (Biotek). Reaction volume per well was 100 µl unless mentioned otherwise. Product concentration was calculated using measured extinction coefficient of para-nitroaniline (pNA) at 405 nm specific for every plate. All curve fitting was done with GraphPad Prism (v7.0e) GraphPad Software, La Jolla California USA, www.graphpad.com.

The time required to obtain maximal stable activator function of SK-plasminogen complex was determined as in [38]. Purified SKs (500 nM) were incubated at 37°C with equimolar concentration of human Lys-plasminogen (Enzyme Research Laboratories) for varying times (0, 5, 15, 20 and 60 min), before being added to wells of a microtiter plate at a final concentration of 5 nM SK-Pg complex in reaction buffer containing 100 nM human Lys-plasminogen and 0.5 mM chromogenic substrate S2251 (H-D-valyl-L-leucyl-L-lysine-*p*-nitroanilide dihydrochloride) (Innovative Research). Absorbance change due to substrate hydrolysis and pNA (i.e. product) formation was measured at 405 nm at 1 min intervals for 20 min. Preincubation for at least 20 min yielded maximal rate of substrate hydrolysis (data not shown) and was used for all subsequent experiments.

Amidolytic assay: The amidolytic activity of all SK variants was measured using previously published protocol with minor modifications.[38–40] Briefly, purified SK (400 nM) was premixed with Lys-plasminogen (200 nM) at 37°C (in a thermocycler) for 20 min to obtain a maximally active SK-Pg complex. The SK-Pg complex thus formed was added to reaction buffer containing varying concentrations of S2251 (100 µM-3 mM) to obtain a final concentration of 20 nM SK-Pg complex. For SK-DNA-Inhibitor complexes reactivated in the presence of DNA, SK-Pg complexes were incubated an additional 20 min at 37°C in the presence of 10-fold excess cDNA. Absorbance changes at 405 nm were monitored for 10 min at 11-13 s intervals and converted to product (i.e. pNA) concentration plotted as a function of time. Slopes of the linear region of this primary time course data (<10% substrate depletion) provided initial rates (k_{obs}), that were plotted against substrate (S2251) concentration. Fitting the latter secondary curve to the Michaelis-Menten equation provided the kinetic parameters (k_{cat} and K_M, Table 1a and Figure S6).

Plasminogen activation: The plasminogen activation ability of the various SK constructs was estimated by determining the kinetic parameters for Lys-plasminogen activation. Preactivated SK-LysPg complex (0.5 nM final concentration) was added to reaction buffer containing 1 mM S2251 and varying concentrations of Lys-plasminogen (22.2-3200 nM). Change in absorbance at 405 nm was measured for up to 40 min at 15-16 s intervals. Kinetic parameters for Lys-plasminogen binding and activation by SK-Pg (k_{cat} and K_M, Table 1b and Figure S6) were determined as described before[40,41] using k_{cat} and K_M of S2251 (Table 1a and Figure S6) obtained for each SK variant.

Functional characterization

Activation of SK constructs: SK (2 µM) was preincubated with Pg (1 µM) at 37°C for 20 min in dilution buffer (50 mM HEPES, pH 7.5, 100 mM NaCl). Complexes generated (SK-LysPg or SK-GluPg) were diluted 10-fold in the same buffer before an additional incubation

for 20 min at 37°C in the presence or absence of trigger cDNA. Reaction was initiated by addition of the activated complex (final concentrations: SK=20 nM and Pg=10 nM) to 1 mM VLK-pNA in reaction buffer and the absorbance monitored at 405 nm for 3 h at 20 s intervals. Concentration of the oligonucleotide complementary to the tether (Table S1) was varied from 1.56-200 nM. Second generation complexes were generated by preincubating Q152C-DE construct with 1.5x or 10x excess of D4-Inhibitor strand for 1 h at room temperature before use and cDNA concentrations were adjusted to 1.56-300 nM or 237-2700 nM respectively, to account for the excess inhibitor strand available. Control reactions with scrambled sequences (Table S1) were performed at highest cDNA concentration tested. All reactions were performed in duplicates, typically with independent protein preparations.

Modified whole blood clot lysis: Fresh blood was collected from normal, healthy donors in sodium citrate vacutainers following IRB protocol (protocol #IRB-17-6930) and used within 4 h. Plasma was obtained from whole blood by centrifugation at 2000xg for 15 min at room temperature. Whole blood clots were prepared as "halos" along the edge of 96-well plates following a protocol previously described[34] with minor modifications as follows (Figure S7a). 5 µl of thrombotic mix made of 300 mM $CaCl_2$ and 48 µg/ml of human alpha-thrombin (Enzyme Research Laboratories) in HBS buffer (20 mM HEPES, pH 7.4, 150 mM NaCl) was applied along the edge of each well. 25 µl of blood mix comprising (40% whole blood and 60% plasma) was added along edge of well to generate a "halo" clot. Plates were sealed and incubated at 37°C for 1 h for fresh clots and 4 h for aged clots formation. Final concentration of components in the clot were: 50 mM $CaCl_2$, 8 µg/ml of human alpha-thrombin, 10% whole blood and 15% plasma. The lower concentration of whole blood used in the assay was to prevent read saturation on the plate reader while keeping the overall clot volume identical to that reported before.[34] Human recombinant tissue-type plasminogen activator (rtPA) was purchased (Innovative Research).

70 µl of 143 nM plasminogen activators (SK variants or rtPA) were overlaid on the clot, reaching a final concentration of 100 nM in 100 µl of clot volume/well. Second generation IDE complexes were generated by preincubating Q152C-DE constructs with 10x excess of D4-Inhibitor for 1 h at RT before use. SK constructs were diluted to 143 nM directly in HBS buffer containing various dilutions of cDNA (or scrDNAs) before immediately adding to clot for monitoring lysis. cDNA concentrations tested were up to 10-fold excess to that of D4-inhibitor strand. Clot lysis over time was measured as the change in absorbance at 510 nm at 30-33 s intervals, with slow shaking for 5 s before each read. Control reactions involving overlaying HBS over clot (A_{zero}) and mixing 30 µl of HBS with 70 µl of blood mix to provide maximum possible absorbance (A_{max}). Thrombus degradation (D(t)) was calculated as: $100*(A(t)- A_{zero})/(A_{max}-A_{zero})$. The time required to reach 50% clot degradation ($T_{0.5}$) was derived from a plot of thrombus degradation versus time. The maximum degradation (D_{max}) is the maximum clot degradation reached over period of the experiment (Figure S7b). A first derivative analysis of the degradation profile provided $D_x(t)/dt$ values over time, t (in min). The maximum clot lysis rate (CLR_{max}) corresponds to the maximum value of $D_x(t)/dt$ achieved during experiment and activation time (A_t) was determined as first value of t for which $Dx(t)/dt > 1$. All reactions were performed as biological duplicates with each replicate involving blood from a different individual.

ASSOCIATED CONTENT

Supporting Information.

Supplementary Information (PDF): Figures S1-S7, Table S1, Supplementary note (containing procedures and compound characterization data for synthesis of inhibitors).

The Supporting Information is available free of charge on the ACS Publications website.

AUTHOR INFORMATION

Corresponding Author

*ghadiri@scripps.edu

NOTES

The authors declare no competing financial interests.

ACKNOWLEDGMENT

We gratefully acknowledge funding from The Skaggs Institute of Chemical Biology, and the American Heart Association postdoctoral fellowship award to P.M. (award ID 17POST32750004) along with support from The Clinical Translational Science Award (CTSA) grant (UL1TR001114). We would like to thank Profs. Colin Longstaff and Christoph Hagemeyer and Dr. Thomas Bonnard for their suggestions and help in establishing the biochemical assays. We would also like to thank our colleagues Prof. Lindsey Miles and Dr. Laurent Mosnier for helpful discussions.

REFERENCES

(1) Marder, V. J.; Aird, W. C.; Bennett, J. S.; Schulman, S.; White, II, G. C. *Hemostasis and thrombosis: Basic Principles and Clinical Practice*; 6th ed.; Wolters Kluwer/Lippincott Williams & Wilkins Health: Philadelphia, 2013.

(2) Mozaffarian, D.; Benjamin, E. J.; Go, A. S.; Arnett, D. K.; Blaha, M. J.; Cushman, M.; Das, S. R.; de Ferranti, S.; Després, J. P.; Fullerton, H. J.; Howard, V. J.; Huffman, M. D.; Isasi, C. R.; Jiménez, M. C.; Judd, S. E.; Kissela, B. M.; Lichtman, J. H.; Lisabeth, L. D.; Liu, S.; Mackey, R. H.; Magid, D. J.; McGuire, D. K.; Mohler, E. R.; Moy, C. S.; Muntner, P.; Mussolino, M. E.; Nasir, K.; Neumar, R. W.; Nichol, G.; Palaniappan, L.; Pandey, D. K.; Reeves, M. J.; Rodriguez, C. J.; Rosamond, W.; Sorlie, P. D.; Stein, J.; Towfighi, A.; Turan, T. N.; Virani, S. S.; Woo, D.; Yeh, R. W.; Turner, M. B.; American Heart Association Statistics Committee; Stroke Statistics Subcommittee; Writing Group Members. *Circulation* **2016**, *133*, e38-360.

(3) Gurman, P.; Miranda, O. R.; Nathan, A.; Washington, C.; Rosen, Y.; Elman, N. M. *Clin. Pharmacol. Ther.* **2015**, *97*, 274–285.

(4) Tate, K. M.; Higgins, D. L.; Holmes, W. E.; Winkler, M. E.; Heyneker, H. L.; Vehar, G. A. *Biochemistry* **1987**, *26*, 338–343.

(5) Petro, M.; Jaffer, H.; Yang, J.; Kabu, S.; Morris, V. B.; Labhasetwar, V. *Biomaterials* **2016**, *81*, 169–180.

(6) Yang, S.; Krug, S. M.; Heitmann, J.; Hu, L.; Reinhold, A. K.; Sauer, S.; Bosten, J.; Sommer, C.; Fromm, M.; Brack, A.; Rittner, H. L. *Biomaterials* **2016**, *82*, 20–33.
(7) Madison, E. L.; Coombs, G. S.; Corey, D. R. *J. Biol. Chem.* **1995**, *270*, 7558–7562.
(8) Schweinitz, A.; Steinmetzer, T.; Banke, I. J.; Arlt, M. J. E.; Stürzebecher, A.; Schuster, O.; Geissler, A.; Giersiefen, H.; Zeslawska, E.; Jacob, U.; Krüger, A.; Stürzebecher, J. *J. Biol. Chem.* **2004**, *279*, 33613–33622.
(9) Nolan, M.; Bouldin, S. D.; Bock, P. E. *J. Biol. Chem.* **2013**, *288*, 29482–29493.
(10) Verhamme, I. M.; Bock, P. E. *J. Biol. Chem.* **2014**, *289*, 28006–28018.
(11) Sawhney, P.; Katare, K.; Sahni, G. *PLoS One* **2016**, *11*, e0155831.
(12) Butcher, K.; Shuaib, A.; Saver, J.; Donnan, G.; Davis, S. M.; Norrving, B.; Wong, K. S. L.; Abd-Allah, F.; Bhatia, R.; Khan, A. *Int. J. Stroke* **2013**, *8*, 560–565.
(13) Kemp, B. E.; Pearson, R. B. *Biochim. Biophys. Acta* **1991**, *1094*, 67–76.
(14) Kobe, B.; Kemp, B. E. *Nature* **1999**, *402*, 373–376.
(15) Hu, S.-H.; Parker, M. W.; Lei, J. Y.; Wilce, M. C. J.; Benian, G. M.; Kemp, B. E. *Nature (London)* **1994**, *369*, 581–584.
(16) Vocero-Akbani, A. M.; Heyden, N. V.; Lissy, N. A.; Ratner, L.; Dowdy, S. F. *Nat. Med.* **1999**, *5*, 29–33.
(17) Krishnamurthy, V. M.; Semetey, V.; Bracher, P. J.; Shen, N.; Whitesides, G. M. *J. Am. Chem. Soc.* **2007**, *129*, 1312–1320.
(18) Gianneschi, N. C.; Ghadiri, M. R. *Angew. Chem. Int. Ed. Engl.* **2007**, *46*, 3955–3958.
(19) Saghatelian, A.; Guckian, K. M.; Thayer, D. A.; Ghadiri, M. R. *J. Am. Chem. Soc.* **2003**, *125*, 344–345.
(20) Pavlov, V.; Shlyahovsky, B.; Willner, I. *J. Am. Chem. Soc.* **2005**, *127*, 6522–6523.
(21) Peri-Naor, R.; Ilani, T.; Motiei, L.; Margulies, D. *J. Am. Chem. Soc.* **2015**, *137*, 9507–9510.
(22) Law, R. H. P.; Caradoc-Davies, T.; Cowieson, N.; Horvath, A. J.; Quek, A. J.; Encarnacao, J. A.; Steer, D.; Cowan, A.; Zhang, Q.; Lu, B. G. C.; Pike, R. N.; Smith, A. I.; Coughlin, P. B.; Whisstock, J. C. *Cell Rep.* **2012**, *1*, 185–190.
(23) Wang, X.; Lin, X.; Loy, J. A.; Tang, J.; Zhang, X. C. *Science* **1998**, *281*, 1662–1665.
(24) Parry, M. A.; Fernandez-Catalan, C.; Bergner, A.; Huber, R.; Hopfner, K. P.; Schlott, B.; Gührs, K. H.; Bode, W. *Nat. Struct. Biol.* **1998**, *5*, 917–923.
(25) Sazonova, I. Y.; Houng, A. K.; Chowdhry, S. A.; Robinson, B. R.; Hedstrom, L.; Reed, G. L. *J. Biol. Chem.* **2001**, *276*, 12609–12613.
(26) Panizzi, P.; Boxrud, P. D.; Verhamme, I. M.; Bock, P. E. *J. Biol. Chem.* **2006**, *281*, 26774–26778.
(27) Dietrich, W.; Nicklisch, S.; Koster, A.; Spannagl, M.; Giersiefen, H.; van de Locht, A. *Anesthesiology* **2009**, *110*, 123–130.
(28) Saupe, S. M.; Steinmetzer, T. *J. Med. Chem.* **2012**, *55*, 1171–1180.
(29) Saupe, S. M.; Leubner, S.; Betz, M.; Klebe, G.; Steinmetzer, T. *J. Med. Chem.* **2013**, *56*, 820–831.
(30) Chang, P. V.; Prescher, J. A.; Sletten, E. M.; Baskin, J. M.; Miller, I. A.; Agard, N. J.; Lo, A.; Bertozzi, C. R. *Proc. Natl. Acad. Sci. USA* **2010**, *107*, 1821–1826.
(31) Tharp, A. C.; Laha, M.; Panizzi, P.; Thompson, M. W.; Fuentes-Prior, P.; Bock, P. E. *J. Biol. Chem.* **2009**, *284*, 19511–19521.
(32) Zhang, L.; Gong, Y.; Grella, D. K.; Castellino, F. J.; Miles, L. A. *J. Thromb. Haemost.* **2003**, *1*, 1264–1270.
(33) Ponting, C. P.; Holland, S. K.; Cederholm-Williams, S. A.; Marshall, J. M.; Brown, A. J.; Spraggon, G.; Blake, C. C. F. *Biochimica et Biophysica Acta (BBA) - Protein Structure and Molecular Enzymology* **1992**, *1159*, 155–161.
(34) Bonnard, T.; Law, L. S.; Tennant, Z.; Hagemeyer, C. E. *Sci. Rep.* **2017**, *7*, 2346.
(35) Reed, G. L.; Kussie, P.; Parhami-Seren, B. *J. Immunol.* **1993**, *150*, 4407–4415.
(36) Steinmetzer, T.; Schweinitz, A.; Stuerzebecher, J.; Steinmetzer, P.; Soefing, A.; Van De Locht, A.; Nicklisch, S.; Reichelt, C.; Ludwig, F.-A.; Schulze, A.; Daghisch, M.; Heinicke, J. US008207378B2, **2012**.
(37) Szabó, G.; Veres, G.; Radovits, T.; Haider, H.; Krieger, N.; Bährle, S.; Miesel-Gröschel, C.; Niklisch, S.; Karck, M.; van de Locht, A. *J. Thorac. Cardiovasc. Surg.* **2010**, *139*, 181–8; discussion 188.
(38) Lin, L. F.; Oeun, S.; Houng, A.; Reed, G. L. *Biochemistry* **1996**, *35*, 16879–16885.
(39) Wohl, R. C.; Summaria, L.; Robbins, K. C. *J. Biol. Chem.* **1980**, *255*, 2005–2013.
(40) Reed, G. L.; Houng, A. K.; Liu, L.; Parhami-Seren, B.; Matsueda, L. H.; Wang, S.; Hedstrom, L. *Proc. Natl. Acad. Sci. USA* **1999**, *96*, 8879–8883.
(41) Huish, S.; Thelwell, C.; Longstaff, C. *PLoS One* **2017**, *12*, e0170936.

Insert Table of Contents artwork here